Chapter Two

Physicochemical properties of Some *Acacia* gums

2.1. Introduction

Carbohydrates embrace more than 90% of the dry weight of all biomass, and more than 90% of the carbohydrate mass is in the form of carbohydrate polymers (polysaccharides). Since these biopolymers are copious, come from renewable sources, are, relatively, inexpensive, are non-toxic, and are amenable to both chemical and biochemical modification, it is not astonishing that they find pervasive and extensive use. For instance, the annual industrial depletion of polysaccharides in the US is ca. 3 000 000 tons with a growth rate of 3% per year. The value of this market is more than 3 trillion dollars. The term 'gum' most often specifically denotes a group of industrially useful polysaccharides (glycans) or their derivatives that hydrate in hot or cold water to form viscous solutions or dispersions at low concentrations. When used in foods, gums are sometimes referred to as hydrocolloids. Gums are classified as natural and modified gum. Natural gums include seaweed extracts (e.g. alginates), plant exudates (e.g. Arabic and Tragacanth gums), gums from seed or root (e.g. potato starch), and gums obtained by microbial fermentation (e.g. gum xanthan). Modified gums include, mostly, cellulose and starch derivatives, such as ethers and esters of cellulose.

Owing to the salable usefulness of gums, physicochemical characterization of these polysaccharides is of substantial importance.

International specification identifies gum arabic as a dried exudate obtained from the stems and branches of *Acacia senegal* var. *senegal* (L.) Willd. or *Acacia seyal* var. *seyal*. The vast majority of gum arabic that enters international trade originates from an area described as 'gum belt' in Sub-Saharan Africa. This belt extends from the northern parts of West Africa eastwards to Sudan, Ethiopia, Eritrea and Somalia (Chikamai, 1998). Gum arabic is used in several industrial applications including food industry (Cossalter, 1991). However, because of the rigorous regulations imposed on all food additives, gum arabic is subject to extensive quality and toxicological controls by countries, organizations and users of the produce. To conform to these requirements and get into market, gum arabic of commerce must fulfill certain chemical specifications (Seif elDin and Zarroug, 1996). The quality of gum arabic is affected by botanical origin, individual tree differences, environmental factors such as climatic and soil conditions, and harvest and post-harvest handlings (FAO, 1995). It is obvious that gums from different species (*Acacia senegal* var. *senegal* and *Acacia seyal* var. *seyal*) exhibited characteristics that are, intrinsically, different. Even within the same species, different varieties and individuals of different provenances produce gum with different characteristics. Recognizing these differences in the species, varieties and

environment is important in producing gum arabic for a desired end use (Chikamai, 1998; Yebeyen, Lemenih, and Feleke, 2009). *Acacia* gums are unique among the various hydrocolloids in that they are water soluble. They are used, notably, in food industry because they modify and control the rheological properties of aqueous food systems acting as thickeners, stabilizers, film formers, suspending agents, flocculants and emulsifiers. *Acacia senegal* var. *senegal* gum is the most widely used in food applications, mainly, because of its better emulsifying properties as *Acacia seyal* var. *seyal* gum (Elmanan, Al-Assaf, Phillips, and Williams, 2008). In addition, gum solutions of *Acacia senegal* var. *senegal* are, generally, less colourful than *Acacia seyal* var. *seyal*. These properties explain differences in the higher price of *Acacia senegal* var. *senegal* gum compared to *Acacia seyal* var. *seyal* in the international market(Vanloot, Dupuy, Guiliano, and Artaud, 2012).

African commercial *Acacia* gums fall into two taxonomic series, *Gummiferae* Benth (subgen *Acacia vas*.) and *Vulgares* Benth: (subgen *Aculeiferum vas*.) as originally proposed by Bentham in 1850 and subsequently refined by others (Jurasek, Varga, and Phillips, 1995; Ross, 1979). *Acacia senegal* var. *senegal* is from the *Vulgares* series and *Acacia seyal* var. *seyal* is from the *Gummiferae* series but in regulatory terms both are considered to be “gum arabic”. The Codex Alimentarius Commission at its 23rd Session in Rome, 28 June- 3July 1999

adopted the following substantive definition of gum arabic "Gum arabic is a dried exudation obtained from the stems and branches of *Acacia senegal* (L) or *Acacia seyal* from *Leguminosae* family" (Dondaina and Phillips, 1999; FAO, 1999; Nie et al., 2013a). There are important differences between the two species of gum arabic which can be summarized as follows (Siddig, Osman, Al-Assaf, Phillips, and Williams, 2005):

Acacia seyal (Gummiferae)	***Acacia senegal (Vulgares)***
Positive optical rotation.	Negative optical rotation.
Less acidic.	More acidic.
Less viscous.	More viscous.
Arabinose/galactose ratio > 1.	Arabinose/galactose ratio <1.
Low rhamnose.	High proportion of rhamnose.

2.1.1. Physicochemical properties of gums

The identification of a particular gum from a series of different gum exudates needs an extensive number of analytical tests to perform. This approach enables "a chemical finger print" of each gum to be determined. The five most important parameters that can be used to identify raw gums are: (1) Specific optical rotation, (2) Nitrogen content, (3) Ash content, (4) Moisture content and (5) Absence of tannins (Karamalla, 1999). The most fundamental properties of a gum which makes it unique amongst polysaccharide, generally, are its solubility and viscosity.

The majority of gums dissolve in water at different concentrations; gum arabic readily dissolves in cold and hot water in concentrations up to 50% (Hassan, 2000; Karamalla, 1999).

2.1.1.1. Moisture content

Moisture content of the gum determines its hardness and hence the variability of densities and the amount of air entrapped during nodule formation. It is determined by measuring the weight loss after evaporation of water. Reducing the moisture content of the natural gum can be readily used as a tenable method of reducing the microbial counts. (Karamalla, 1999).

2.1.1.2. Ash content

The ash content indicates the presence of inorganic elements existing in salt form. (Karamalla, Siddig, and Osman, 1998) and Karamalla (1999) showed that the type of soil (clay or sand) affects the ash content significantly.

2.1.1.3. pH value

The hydrogen ion concentration plays an important role in the chemistry and industrial use of gums. The change in the concentration of hydrogen ion may determine the solubility of gum and the precipitation of protein, therefore functional properties of a gum may be affected by change in pH for example viscosity and emulsifying power. Crude gum Arabic is slightly acidic because of

the presence of few free carboxyl groups of its constituent acidic residues, D-glucuronic acid and its 4-O-methy1 derivatives.

2.1.1.4. Specific optical rotation

The optical activity of organic molecules (saccharides and carbohydrates) is related to their structure and is a characteristics property of the substance, and thus the specific rotation is considered as the most important criterion of purity and identity of any type of gum.

2.1.1.5. Nitrogen and protein content

The role of nitrogen and nitrogenous component in the structure, physicochemical properties and functionality of gum arabic was subjected to intensive investigation (Dickinson *et al.,* 1988)(Randall, Phillips, and Williams, 1989). Dickinson, Galazka, and Anderson (1991), studied the emulsifying behavior of gum arabic and concluded that there was a strong correlation between the proportion of protein in the gum and emulsifying stability.

The micro Kjeldahl method was used to determine the total nitrogen in gum samples; the nitrogenous compound was digested with concentrated sulphuric acid in the presence of copper sulphate-potassium sulphate catalyst to yield ammonium sulphate. An excess of sodium hydroxide is added and ammonia is distilled in steam, absorbed in boric acid and titrated with hydrochloric acid using methyl red as indicator. The reactions involved in these steps are shown as follows;

- Sample + H_2SO_4 (conc.) catalyst +Heat → $(NH_4)_2SO_4$
- $(NH_4)_2SO_4$ + 2 Na OH → $2NH_3 + Na_2SO_4 + 2H_2O$
- $NH_3 + H_3BO_3 \rightarrow NH_4^+ + H_2BO_3^-$
- $H_2BO_3^- + HCl \rightarrow H_3BO_3 + Cl^-$

2.1.1.6. Number average molecular weight

An important group of absolute methods allowing the determination of the molecular weight of macromolecules is based on the measurement of colligative properties. Here, the activity of the solvent is measured in a polymer solution via determination of the osmotic pressure π_{os}. The value of π_{os} required to determine the number-average molecular weight can be obtained using a membrane osmometer. Here, in a measuring cell having two chambers separated by a semi permeable membrane, one chamber contains the pure solvent and the second one the polymer solution in the same solvent (a membrane is called semi permeable if only the solvent can pass through but not the polymer molecules). Due to the lower activity (lower chemical potential) of the solvent in the polymer solution as compared to the pure solvent, solvent molecules migrate through the membrane from the solvent chamber into that of the polymer solution and dilute it. Therefore, the volume of the polymer solution increases until an equilibration is reached between the osmotic pressure π_{os} and the hydrostatic pressure generated by the diluted polymer solution.

$$\pi_{os} = \sigma\, g\, \Delta h \quad \text{…………………………………………… (2.1)}$$

Where σ is the density of the solvent and *g* is the acceleration of gravity. Following Van't Hoff, it is

$$\pi_{os}\, V = nRT \quad \text{…………………………………………….. (2.2)}$$

For diluted solutions, with *V* being the volume of the polymer solution and *n* the number of moles of the dissolved polymer. Since $n = m/M_n$ (*m* is the mass (in g) of dissolved polymer) and $c = m/V$ it follows that:

$$\pi_{os} = \frac{m}{V}\frac{RT}{M_n} = \frac{cRT}{M_n} \quad \text{…………………………………… (2.3)}$$

Since Van's Hoff's law is valid only for infinitely diluted solutions, one develops π_{os}/c in power law series (break after the linear term in c)

$$\frac{\pi_{os}}{c} = \frac{RT}{M_n} + A_2 . c \quad \text{…………………………………… (2.4)}$$

Thus, the osmotic pressure is first measured at different polymer concentrations, π_{os} / c is then plotted vs. c, the values are linearly extrapolated to $c \to 0$, and the value of M_n is determined from the *y* axis intercept. A_2 is the second virial coefficient of the osmotic pressure.

If the solvent is good enough or the concentration is high enough then the $\mathbf{c^2}$ term is significant, the points may deviate from a straight line. In such cases It is useful to plot $(\pi/c)^{1/2}$ versus c as suggested by equations:

$$(\pi/c)^{1/2} = \left(RT/M_n\right)^{1/2} (1 + \Gamma/2\, c) \text{ .... (2.5)}$$

Since

$$\Gamma = A_2/A_1 \;\; and\; A_{1=}\, 1/M_n$$

We can write

$$(\pi/c)^{1/2} = \left(RT/M_n\right)^{1/2} + \left(RT/M_n\right)^{1/2} A_2\, M_n/2\, c \text{..................... (2.6)}$$

$$\text{The intercept} = \left(RT/M_n\right)^{1/2} \text{ ....(2.7)}$$

$$\text{The slope} = \left(RT/M_n\right)^{1/2} A_2\, M_n/2 \text{ ....(2.8)}$$

If the second virial coefficients equal zero, the solvent is considered ideal. The better solvent has the higher value of A_2.

For an ideal solvent, $A_2 = 0$

For good solvent, $A_2 > 0$

For poor solvent, $A_2 < 0$ (Tager, 1978).

According to statistical mechanical solution theory, A_2 represents the interaction of a single solute particle with the solvent, and higher order virial coefficients are associated with, correspondingly, larger number solute particle cluster interactions with the solvent. For membrane Osmometer (as well as for all other techniques of

molecular weight determination via colligative properties) it is very important that the samples to be analyzed are very pure. In particular low-molecular-weight impurities have to be removed. Otherwise, they will migrate through the semi permeable membrane and lower the chemical potential of the solvent in the reference chamber. An overestimation of the molecular weight will follow. The same effect applies when there are very small oligomers in the test sample.

2.1.2. Nuclear Magnetic Resonance (NMR)

Nuclear magnetic resonance (NMR) spectroscopy is based on the measurement of absorption of electromagnetic radiation in the radio-frequency region of, roughly, 4-900 MHz In contrast to UV, visible, and IR absorption, nuclei of atoms rather than outer electrons are involved in the absorption process. Furthermore, to cause nuclei to develop the energy states required for absorption to occur, it is necessary to place the analyte in an intense magnetic field(Holler, Skoog, and Crouch, 2007). NMR spectroscopy is a powerful analytical technique that is often employed to study polymers. The detailed structural information obtained from NMR is, frequently, not available through other analytical techniques. Over the years, numerous publications have appeared on the NMR of food polysaccharides, and NMR has become a routine method of analysis (Cheng and Neiss, 2012).

2.1.3. ATR-FTIR Spectroscopy

The technique of Attenuated Total Reflectance (ATR) has, in recent years, revolutionized solid and liquid sample analysis because it combats, the most challenging, aspects of infrared analyses, namely sample preparation and spectral reproducibility. An attenuated total reflection accessory operates by measuring the changes that occur in a, totally, internally reflected infrared beam when the beam comes into contact with a sample (Figure 2.1). An infrared beam is directed onto an optically dense crystal with a high refractive index at a certain angle. This internal reflectance creates an evanescent wave that extends beyond the surface of the crystal into the sample held in contact with the crystal. It can be easier to think of this evanescent wave as a bubble of infrared that sits on the surface of the crystal. This evanescent wave protrudes, only, a few microns (0.5 - 5) beyond the crystal surface and into the sample. Consequently, there must be good contact between the sample and the crystal surface. In regions of the infrared spectrum where the sample absorbs energy, the evanescent wave will be attenuated or altered. The attenuated energy from each evanescent wave is passed back to the IR beam, which then exits the opposite end of the crystal and is passed to the detector in the IR spectrometer. The system then generates an infrared spectrum. For the technique to be successful, the following two requirements must be met:

• The sample must be in direct contact with the ATR crystal, because the evanescent wave or bubble only extends beyond the crystal 0.5 - 5 .

• The refractive index of the crystal must be, significantly, greater than that of the sample or else internal reflectance will not occur– the light will be transmitted rather than, internally, reflected in the crystal. Typical ATR crystals have refractive index values between 2.38 and 4.01 at 2000 cm^{-1}.It is safe to assume that the majority of solids and liquids have much lower refractive indices.

The ATR-FTIR contains an ATR crystal through which an infrared (IR) beam passes. The sample that does not need any preparation is placed on the surface on top of the crystal. The ATR-IR beam passes through the crystal and by total reflection an evanescent wave is formed. The evanescent wave extends through the sample and absorption of energy by the sample can occur. In that case the energy of the evanescent wave debilitates. All waves are returned to the infrared beam that goes to the detector. The obtained spectra can be compared with reference spectra (Buggenhout, 2014).

2.1.4. Thermal analysis

Thermal analysis techniques are those in which a physical property of a substance or its reaction products is measured as a function of temperature. Usually the substance is subjected to a controlled temperature program during the analysis(Holler et al., 2007). Although there are more than a dozen thermal

analysis techniques, the discussion in this chapter will be confined to two methods; **Differential Scanning Calorimetry (DSC)** and **Thermogravimetric Analysis (TGA)**. Phase transitions in foods are often a result of changes in composition or temperature during processing or storage. Knowledge of transition temperatures and of the thermodynamic quantities is important to understand the processes such as: dehydration, evaporation, freezing and conservation(Mothé and Rao, 2000).

2.1.4.1. Differential Scanning Calorimetry (DSC)

DSC has emerged as powerful physical tool to monitor physical and chemical changes that occur in the polysaccharide during thermal processing and these methods yield curves that are unique for a given polysaccharide(Bothara and Singh, 2012). DSC is the most often used analysis method, primarily because of its speed, simplicity, and availability. In DSC a sample and a reference are placed in holders in the instrument. Heaters either ramp the temperature at a specified rate (e.g., 5°C/min) or hold the DSC at a given temperature. The instrument measures the difference in the heat flow between the sample and the reference. DSC is a calorimetric method in which differences in energy are measured (Figure 2.2).

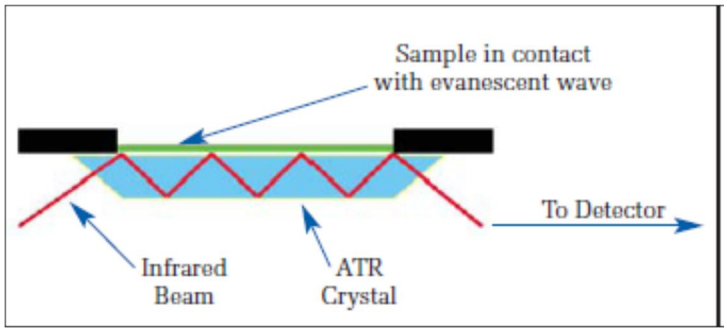

Figure (2.1): A multiple reflection ATR system.

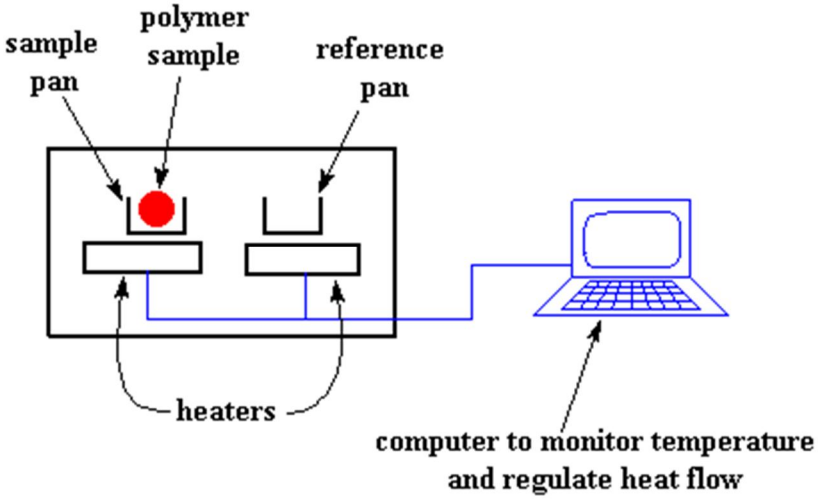

Figure (2.2): The workings of a DSC machine.

Figure (2.3): ASG, AMF, ASY, and ATR Gums nodules.

During the heating of a sample from room temperature to its decomposition temperature, peaks with positive and negative ΔdH/dt may be recorded; each peak corresponds to a heat effect associated with a specific process, such as crystallization or melting. The question arises as to what kind of information is obtainable from a DSC curve. The first and most direct information is the temperature at which a certain process occurs, for example, the melting point of a polymer. The temperature at which a reaction, such as decomposition, may start is another important parameter. The peak temperature is associated with the temperature at which maximum reaction rate occurs. A special case in which the temperature of a phase transformation is of great importance in polymers is the glass transition temperature, T_g. This is the temperature at which amorphous (noncrystalline) polymers are converted from a brittle, glasslike form to a rubbery, flexible form. This is not a true phase transition but one that involves a change in the local degrees of freedom. Above the glass transition temperature certain segmental motions of the polymer are comparatively unhindered by the interaction with neighboring chains. Below the glass transition temperature, such motions are hindered greatly, and the relaxation times associated with such hindered motions are usually long compared to the duration of the experiment.

DSC finds many applications in characterizing materials. Quantitative applications include the determination of heat of fusion and the extent of crystallization for

crystalline materials. Glass transition temperatures and melting points are useful for qualitative classification of materials, although thermal methods cannot be used alone for identification. Melting points are also very useful in establishing the purity of various preparations. Hence, thermal methods are often used in quality control applications.

At the glass transition, the polymer undergoes changes in volume and expansion, heat flow and heat capacity. The change in heat capacity is readily measured by DSC. With crystalline materials, the level of crystallinity is an important factor for determining polymer properties. Degrees of crystallinity can be determined by IR spectroscopy, X-ray diffraction, density measurements, and thermal methods. In most cases DSC is one of the easiest methods for determining levels of crystallinity. The crystallinity level is obtained by measuring the enthalpy of fusion for a sample $(\Delta H_f)_{sample}$ and comparing it to the enthalpy of fusion for the fully crystalline material $(\Delta H_f)_{crystal}$. Calorimetric methods are also used to study crystallization rates. Crystallization is an exothermic event, the rate of heat release and thus the crystallization kinetics can be followed by DSC(Holler et al., 2007).

2.1.4.2. Thermogravimetric Analysis (TGA)

Thermogravimetric analysis (TGA) is a simple and accurate method for studying the decomposition pattern and the thermal stability of polymers(Bothara and Singh, 2012). In TGA the mass of a sample in a controlled atmosphere is recorded,

continuously, as a function of temperature or time as the temperature of the sample increased (usually linearly with time). A plot of mass or mass percentage as a function of time is called thermogram or a thermal decomposition curve.

TGA instruments consist of (1) a sensitive microbalance, called a thermobalance; (2) a furnace; (3) a purge-gas system for providing an inert, or sometimes reactive, atmosphere; and (4) a computer system for instrument control, data acquisition, and data processing. A purge-gas switching system is a common option for application in which the purge gas must be changed during an experiment.

Because TGA monitors the mass of the analyte with temperature, the information provided is quantitative, but limited to decomposition and oxidation reactions and to such physical processes as vaporization, sublimation, and desorption. Among the most important applications of TGA are composition and decomposition profiles of multicomponent systems. In polymer studies, thermograms provide information about decomposition mechanisms for various polymeric preparations. In addition, the decomposition patterns are characteristic for each kind of polymer and can sometimes be used for identification purposes(Holler et al., 2007).

The objective of this work is to authenticate some *Acacia* gums samples namely *Acacia senegal* var. *senegal* and *Acacia mellifera* from the *Vulgares* series and *Acacia seyal* var. *seyal* and *Acacia tortilis* var.*raddiana* from the *Gummiferae*

series using different physicochemical methods, NMR spectroscopy, FTIR, and thermal analysis; DSC and TGA.

2.2. Materials and methods

2.2.1. Materials

Acacia senegal var. *senegal* gum (ASG) was provided by Dr. M. E. Osman, Natural Gums Research Centre of Sudan University of Science and Technology, (season 2013). *Acacia seyal* var. *seyal* gum (ASY) was provided by Dr. E. A. Hassan. *Acacia mellifera* gum (AMF) was provided by Gum Arabic Research Center P.O.Box 160 El Obied Sudan. *Acacia tortilis* var. *raddiana* gum (ATR) was collected from Wad-Mahala Forest 45km south east Khartoum with the assistance of the Forests National Corporation (FNC) Sudan**.** Gums nodules were irregular in shape (Figure 2.3). Isopropyl myristate (IPM) oil from Spectrum Chemical MFG. CORP., 90.0% assay and 0.846-0.854g/ml specific gravity at 25**C**, was used as the dispersed phase. Deionized water (18.2 MΩ cm^{-1}, resistivity) was used throughout this work.

2.2.2. Samples preparations

Gum nodules were dried at room temperature, cleaned by hand, ground using mortar and pestle, and kept in labeled plastic containers for analysis.

2.2.3. Moisture content

The **moisture content** was calculated according to (AOAC, 1990) method. Accurately weighed one gram of the ground gum was heated in an oven (Heraeus) at 105°C to a constant weight. Then, the moisture content was determined as percentage of the lost weight to the total weight as follows;

$$\text{Moisture content (\%)} = \frac{W_1 - W_2}{W_1} \times 100 \quad \ldots\ldots\ldots\ldots\ldots\ldots\ldots\ldots \text{(2.9)}$$

W_1 = Original weight of sample (g).

W_2 = Weight of sample after drying (g).

2.2.4. Ash content

Ash content was determined according to(AOAC, 1990) method. Ash content was determined by weighing the sample (1g) in a pre-weighed ashing dish after heating at 550 **C** for 5 h. The dish was cooled to room temperature in a desiccator and was weighed again. The weight loss was calculated as a percentage of the initial weight taken as follows;

$$\text{Ash (\%)} = \frac{W_3 - W_1}{W_2 - W_1} \times 100 \quad \ldots\ldots\ldots\ldots\ldots\ldots\ldots\ldots\ldots\ldots \text{(2.10)}$$

Where:

W_1 = Weight of the empty crucible (g).

W_2 = Weight of the crucible + the sample (g).

W_3 = Weight of the crucible + ash (g).

2.2.5. Nitrogen and protein content

The nitrogen content was determined according to the Kjeldahl method(AOAC, 1990). (25 ml) of concentrated sulphuric acid were added to 1.5 g of sample. The sample was hydrolyzed and solubilized by heating the mixture to 100 **C** until the solution was clear and greenish. The digest was placed in the Kjeldahl distillation apparatus and the distillate was collected into 3% boric acid solution. The obtained boric acid solution was titrated against 0.01 M hydrochloric acid using Tashiro as indicator. The amount of nitrogen was calculated according to the expression;

$$N[\%] = \frac{V \times 0.1401 \times 100}{1000 \times W} \quad \text{...} \quad (2.11)$$

Where V is the amount of 0.01 M HCl (ml) and W is the weight of sample in grams.

Protein content of sample was calculated using nitrogen conversion factor (NCF), of 6.60, for ASG and AMF (Anderson, 1986), 6.625 for ASY (Osman, 1993), and 6.7 for ATR (Abdelrahman, 2011) as follows:

$$\text{Protein } (\%) = \text{N } (\%) \times \text{NCF} \quad \text{..} \quad (2.12)$$

2.2.6. pH Measurement

The pH values were measured directly in a homogenate prepared with 1% (w/v) gum powder (on dry basis) in distilled water, using a JENWAY 3510 pH meter at room temperature.

2.2.7. Specific optical rotation $[\alpha]_D^T$

The specific rotation was measured for 1% (w/v)solution (on a dry basis) using an Optical Activity Bellingham and Stanley Ltd. polarimeter fitted with a sodium lamp and with a cell of path length of 20 cm at 25**C**. The specific optical rotation was calculated according to the relationship:

Specific optical rotation $[\alpha]_D^T = \frac{\alpha \ x \ 100}{L \ x \ C}$ …….. (2.13)

Where:

α = Observed angle of rotation.

L = the length of sample holder in decimeters (dm).

C = concentration in gm/100ml

T = Temperature.

2.2.8. M_n determination from osmotic pressure measurements

The osmotic pressure of gum samples was determined for a series of aqueous solutions on a dry weight basis using OSMOMAT 050 instrument. The lower half of the osmotic cell, which is closed off to the outside, is filled with electrolyte containing ringer's solution. The upper half of the cell, which is open to the outside, is filled with a colloid-containing solution. The two halves of the cell are separated from each other by a semi permeable. This membrane possesses defined pores, through which only water and electrolyte can pass. Due to osmotic pressure differential of the two solutions, solvent permeates from the lower into the upper

half of the measuring cell until equilibrium is reached between the pressure in lower half of the cell and the osmolal concentration. An electronic pressure measuring system, which is mounted into the lower half of the cell, transduces the under pressure into an electronic signal, which is shown on a digital display.

2.2.9. NMR Spectroscopy

Both ^{1}H and ^{13}C spectra were recorded on a JEOL JNM-ECX500 spectrophotometer. All gum samples were dissolved in deuterium oxide (≈2% w/w) at 90 **C** for 3 h before NMR analysis. The spectra of ^{1}H and ^{13}C were measured using a standard single-pulse sequence. The experiments were conducted at 50**C (**Nie et al**.,** 2013b**)**.

2.2.10. ATR-FTIR Spectroscopy

FTIR spectra were obtained using a Perkin-Elmer ATR- FTIR Spectrophotometer. The scanning range was 400 to 4000 cm^{-1} and the resolution was 1 cm^{-1}. After the crystal area was cleaned, the solid material was placed onto the small crystal area; the pressure arm was positioned over the crystal/sample area. Force was applied to the sample, pushing it onto the diamond surface and the spectrum was collected.

2.2.11. Thermal analysis

2.2.11.1. Differential Scanning Calorimetry (DSC)

Instrument: DSC Q20 V24.10 Build 122, Module DSC Standard Cell FC, Pan: T zero Aluminum Hermetic, Nitrogen gas flow rate: 50.0 ml/min. Sample of gum

species (about 5 mg) was placed in a pre-weighed aluminum sample pan and the pan was sealed using a Quick Press pan crimper and the thermal data between 30**C** to 400**C** in nitrogen atmosphere with a heating rate of 10**C** min^{-1} was recorded. An empty pan served as the reference.

2.2.11.2. Thermogravimetric Analysis (TGA)

Thermogravimetric analysis (TGA) is second only to differential scanning calorimetry (DSC) as the most widely spread thermoanalytical measuring method. It measures mass change as a function of time or temperature, thereby subjecting the sample to a defined and controlled environment (heating rate, gas atmosphere, flow rate, crucible type, etc.). A thermobalance is employed for measuring the quantitative composition of a polymer compound or a blend. Mass loss in inert gas atmospheres occurs as a result of processes such as the release of water or moisture (drying behavior), the emission of solvents and plasticizers, or the decomposition of polymers, temporally differentiated according to thermostability properties.

Thermogravimetric analysis (TGA) is a simple and accurate method for studying the decomposition pattern and the thermal stability of polymers(Vinod and Sashidhar, 2009). The instrument: NETZSCH, TG 209 F3 Tarsus runs under Proteus® Software on Windows® operating system. About 13mg of gum samples were weighed in sample pans and the weight loss against temperature from ambient to 400**C** at a heating rate of 10**C** min^{-1} was recorded.

2.3. Results and discussions

2.3.1. Physicochemical Properties

Table (2.1) shows analytical data of the samples under the study. Analysis of samples was carried out in triplicate and then averaged.

The physicochemical properties for the *Acacia* species fall within the range of the specifications of the gums reported byKaramalla et al. (1998) for ASG gum. For AMF gum the analytical parameters agree well with that reported by Al-Assaf, Phillips, and Williams (2005) and that reported by Hassan, Al-Assaf, Phillips, and Williams (2005) and that reported by Elmanan et al. (2008) for ASY gum. The results were in a good agreements with findings of Abdelrahman (2011) for ATR gum.

2.3.2. Nuclear Magnetic Resonance (NMR)

Figures (2.3-2.8) and (2.9-2.12) show ^{13}C and ^{1}H NMR spectra of *Acacia* polysaccharide gums (ASG, AMF, ASY, and ATR) respectively. Representative ^{1}H and ^{13}C chemical shifts for polysaccharides were listed in Table (2.2) below.

Typical NMR spectra were reported for ASG (Nie et al., 2013b) and for ASY (Nie et al., 2013a).

Table 2.1. Physiochemical properties of gums.

Gum	Moisture (%)	Ash (%)	Nitrogen (%)	Protein (%)	pH	Sp.Opt.Rotation	$M_n x10^6$
ASG	9.76	3.40	0.327	2.158[1]	4.94	- 31.75	0.24
AMF	9.56	2.50	0.630	4.158[1]	4.53	- 48.25	2.10
ASY	8.35	3.13	0.243	1.610[2]	4.84	+56.00	2.95
ATR	8.49	2.05	1.549	10.378[3]	4.45	+86.75	2.06

[1] 6.6 NCF(Anderson, 1986),[2]6.625 NCF(Osman, 1993), [3]6.7 NCF(Abdelrahman, 2011)

Table 2.2. Representative ^1H and ^{13}C chemical shifts for nuclei of polysaccharides [a,b].

^1H	shift (ppm)	^{13}C	shift (ppm)
CH_3C	~1.5	CH_3C	~15
CH_3CON	1.8–2.1	CH_3COH)	20–23
CH_3CO_2	2.0–2.2	CH_3CO_2)	
CH(NH)	3.0–3.2	CH_2C	38
CH_3O	3.3–3.5	CH_3O	55–61
H-2 to H-6′	3.5–4.5	CH(NH)	58–61
H-5	4.5–4.6	CH_2OH	60–65
H-1 (ax)	4.5–4.8	C-2 to C-5	65–78
$H\text{-}C(OH)_2$	5.2	C-X[c]	78–87
HO	5.0–5.4	C-1 (ax-O, red)	90–95
H-1 (eq)	5.3–5.7	C-1 (eq-O, red)	95–98
$H\text{-}CO_2$	5.9	C-1 (ax-O, glyc)	98–103
		C-1 (eq-O, glyc)	103–106
		C-1 (fur)	106–109
		COOH	174–175
		COOR	175–180

	Substituent effects on α-^1H and α-^{13}C (ppm)[d],			
	O-Alkyl	O-Acyl	O-Sulfate	O-Phosphate
^1H	–0.2–0.3	+0.3–0.5	+0.3–0.6	+0.3–0.5
^{13}C	+7–10	+<3	+6–10	+2–3

[a] (Cheng and Neiss, 2012)
[b] Abbreviations: ax, axial; eq, equatorial; red, reducing; glyc, glycosidic; fur, furanosyl.
[C] Non-anomeric ^{13}C involved in glycosidic linkage.
[d] Downfield, +; upfield, -.

2.3.2.1. ^{13}C Nuclear Magnetic Resonance (NMR)

^{13}C NMR spectrum of ASG (Fig. 2.4&2.5) showed the non-anomeric carbons C_2-C_5 and the anomeric carbons of monosaccharide components respectively. Figures (2.6-2.9) showed ^{13}C spectra of ASG, AMF, ASY, and ATR gums, the peaks at 16.96, 16.91, 16.21, and 16.95 ppm respectively, belong to the carbon of methyl group of rhamnose, and for each gum the peaks at around 175 ppm are typical C-6 signal of an uronic acid. These results are consistent with the finding of Nie et al. (2013b).

^{13}C NMR spectrum also indicates that the gums contain deoxygenated sugars. This is evident from the $-CH_3$ signals appearing in the much higher field 15 to 20 ppm (Cui, 2005). This $-CH_3$ is attributed to the methyl group of rhamnose sugar units. The signal between 20 to 30 ppm is thought to be a $-CH_2$ linked to OH which pushes the signal, slightly, downfield. The CH_2OH may be attributed to the glucose sugar unit. Signals from anomeric carbons of the monosaccharide components appear in the 90 to 110 ppm (Cui, 2005). The α- anomeric carbons are seen in the region of 95 to 103 ppm showing about 5 anomeric carbons which may be attributed to the five neutral sugar components of the polysaccharide while the signals due to non-anomeric carbons C_2-C_5 appear between 60 to 85 ppm (Nep and Conway, 2010).

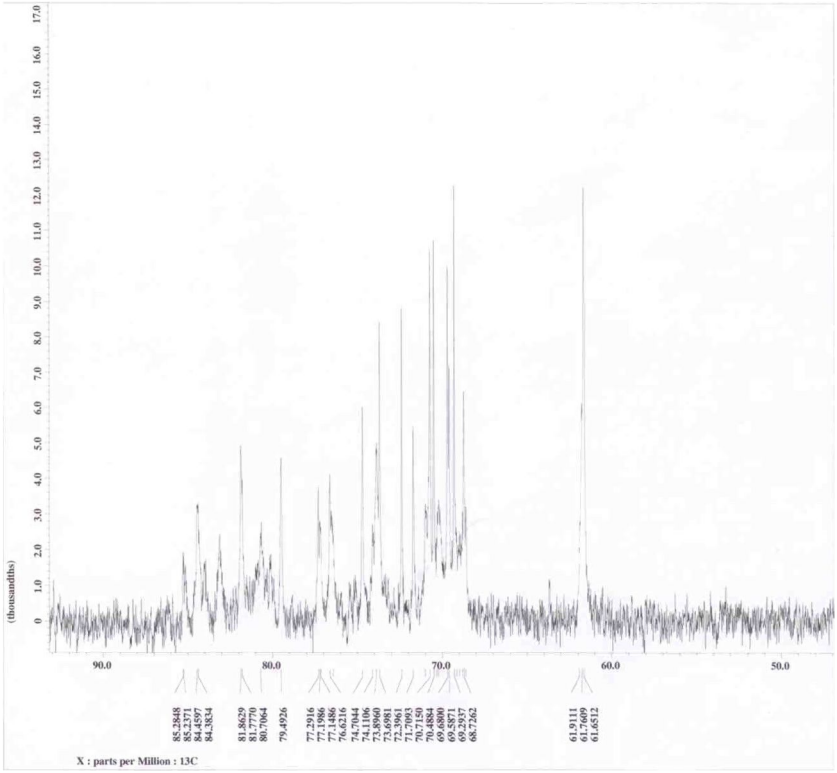

Figure (2.4): ASG Gum ^{13}C NMR Spectrum of non-anomeric carbons C_2-C_5.

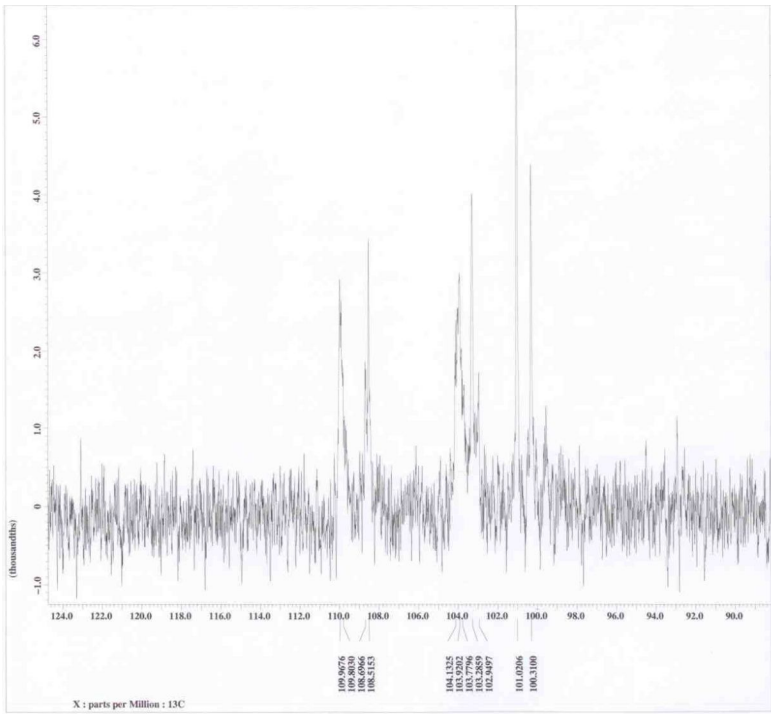

Figure (2.5): ASG ^{13}C NMR Spectrum of anomeric carbons of the monosaccharide.

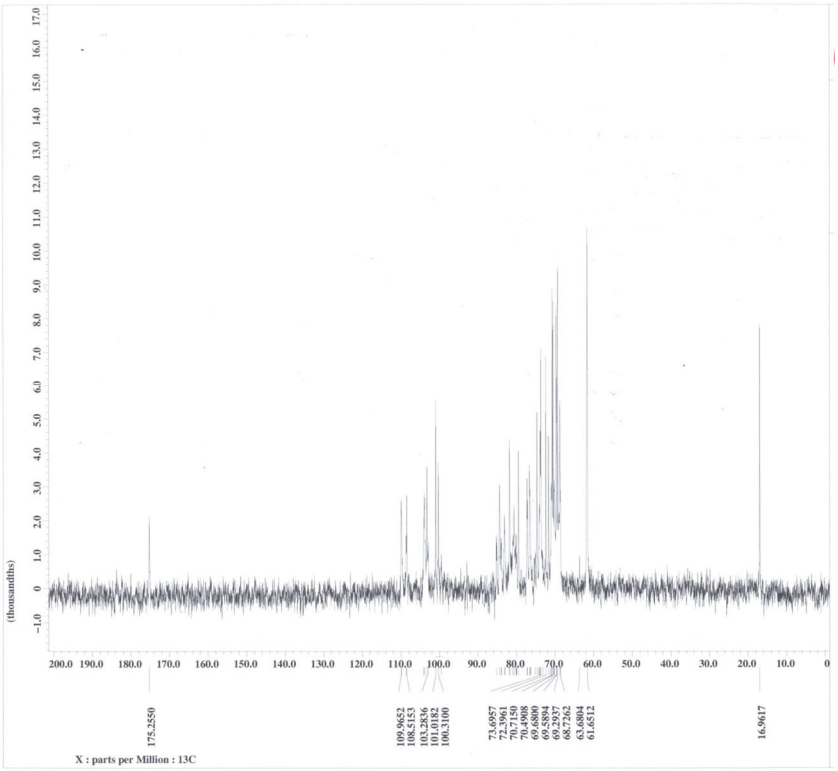

Figure (2.6): ASG Gum ^{13}C NMR Spectrum.

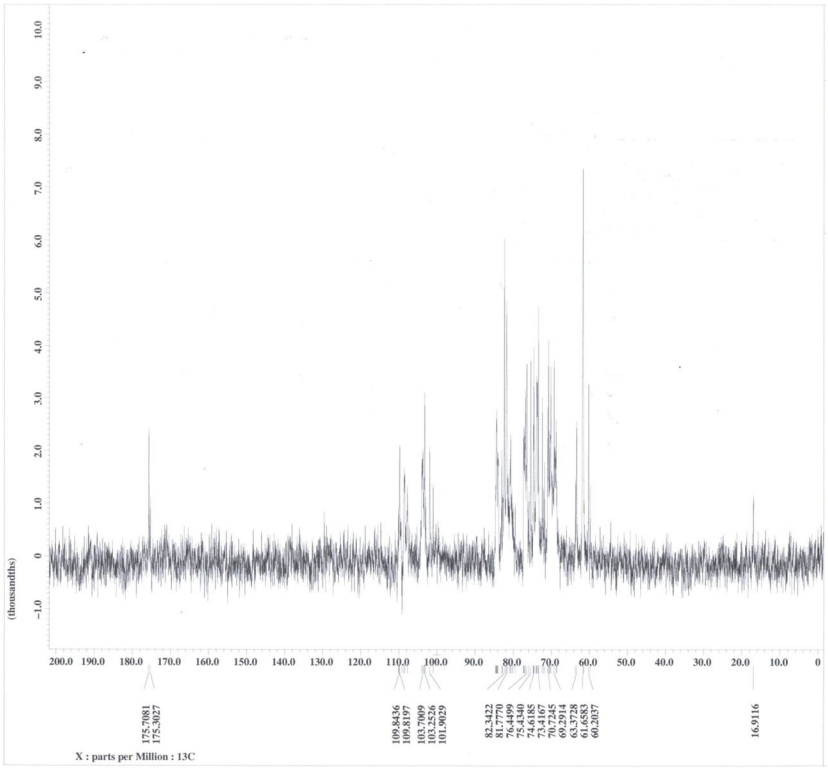

Figure (2.7): AMF Gum ^{13}C NMR Spectrum.

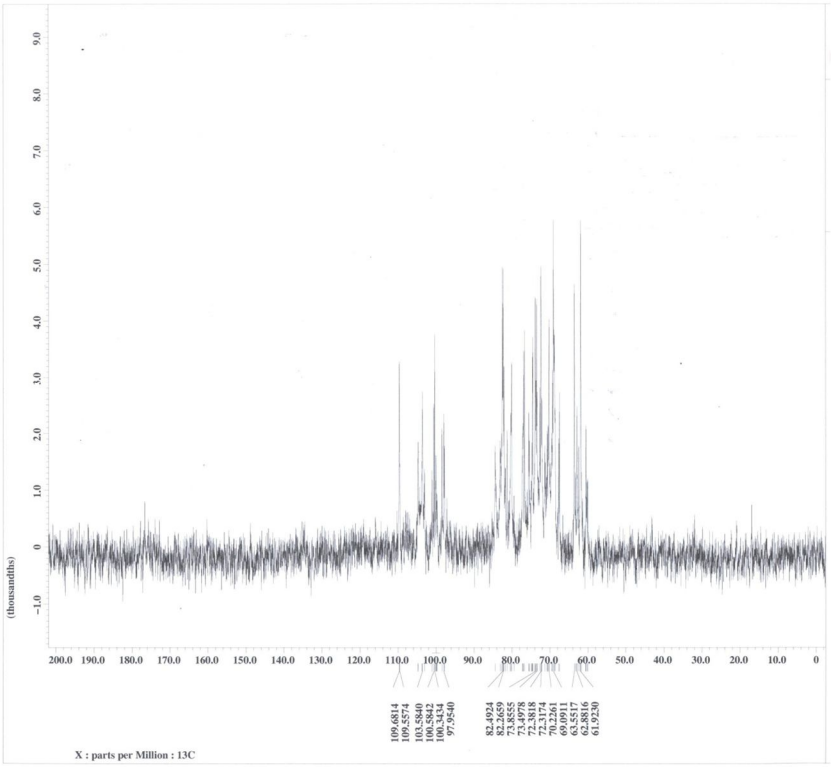

Figure (2.8): ASY Gum ^{13}C NMR Spectrum.

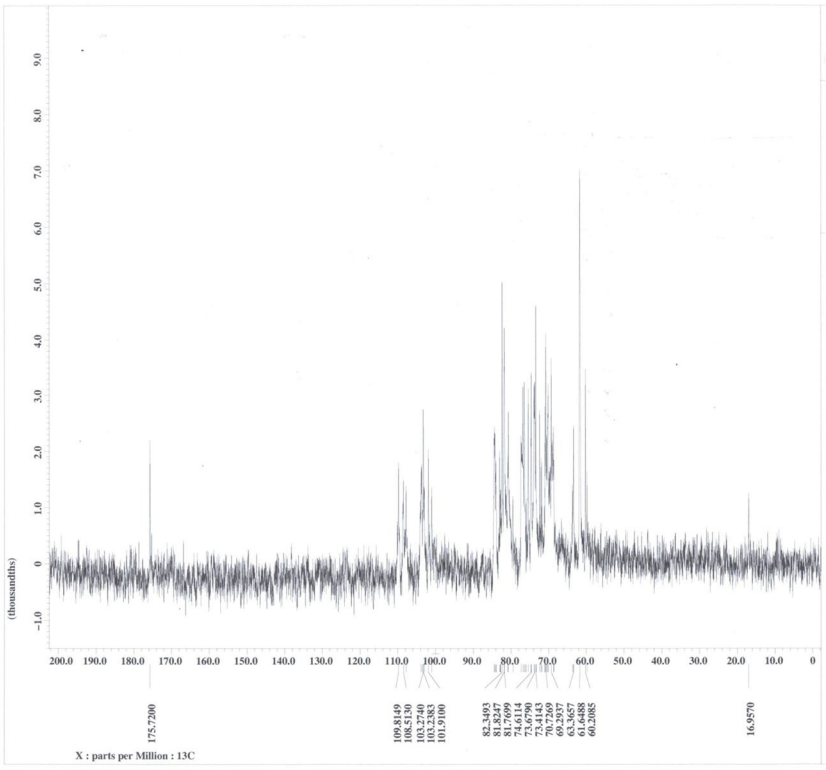

Figure (2.9): ATR Gum ^{13}C NMR Spectrum.

2.3.2.2. ^{1}H Nuclear Magnetic Resonance (NMR)

Figures (2.10-2.13); show the ^{1}H NMR spectra of the gum samples (ASG, AMF, ASY, and ATR). More than ten peaks can be observed clearly in the anomeric region (3.5-5.8 ppm) in the ^{1}H NMR spectrum of the gums. The peak at 1.41, ppm can be assigned to the methyl group of rhamnose. Dominant peaks are identified at 5.65, 5.55, 5.46, 4.92 and 4.87 ppm. The high intensity peak at 4.6-4.80 ppm is partially due to the presence of H_2O. The ^{1}H NMR spectrum is crowded in a narrow region between 3 to 5 ppm typical of polysaccharides and confirms the presence of many similar sugar residues. The ^{1}H NMR spectrum of ASY and ATR gums showed an upfield proton chemical shift at 2.13 ppm indicate that an acetyl group ($COOCH_3$)is present (Nie et al., 2013a). The signals between 3.91 to 4.74 ppm can be assigned to non-anomeric protons (H_2- H_6) while signals between 4.3 to 4.8, and 4.92 to 5.64 ppm arise from β-anomeric and α-anomeric protons respectively (Glicksman and Schachat, 1959). The signals between 3.0 to 3.8 ppm have also been assigned to -O-CH_3. Again, the -CH_3 indicates the presence of methylated sugar (rhamnose) and agrees with the ^{13}C NMR(Nep and Conway, 2010).

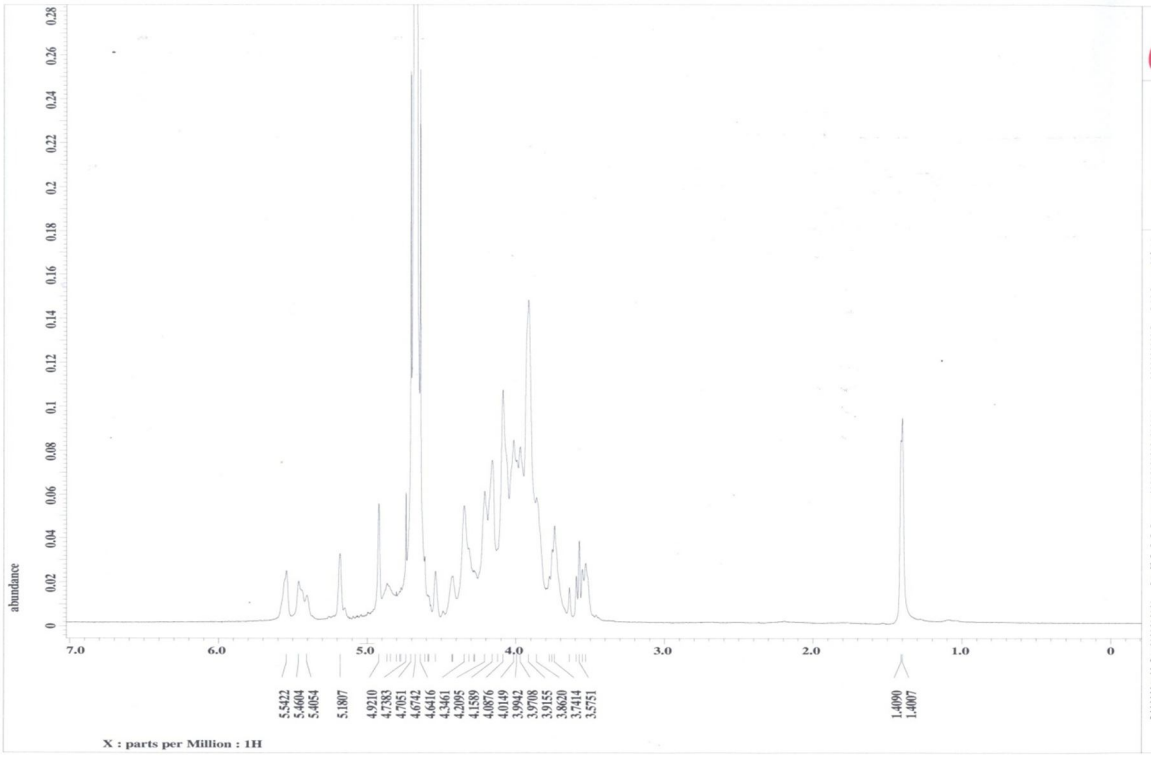

Figure (2.10): ASG Gum ^{1}H NMR Spectrum.

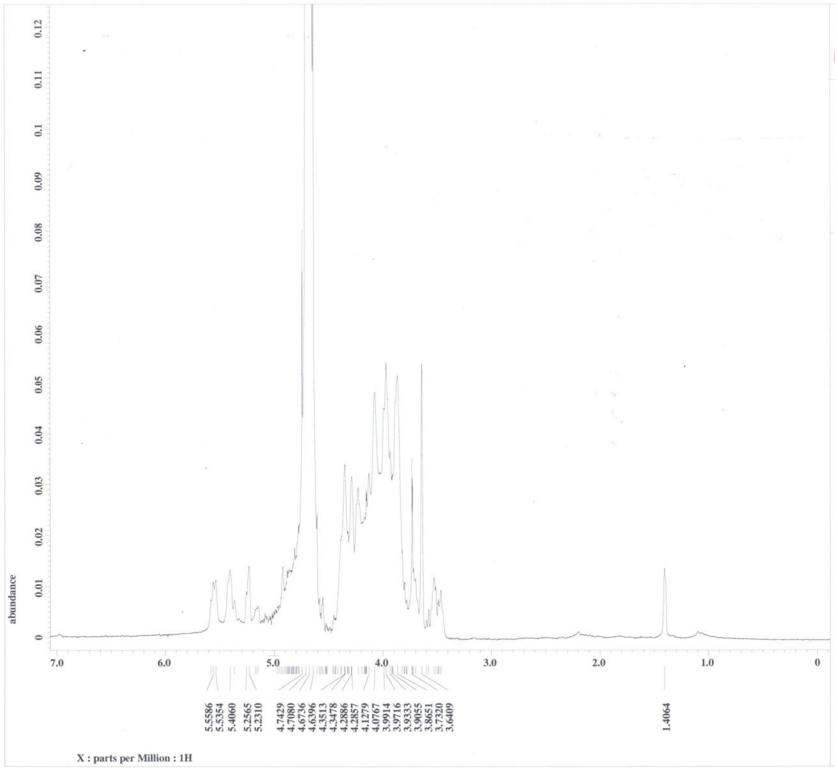

Figure (2.11): AMF Gum ^{1}H NMR Spectrum.

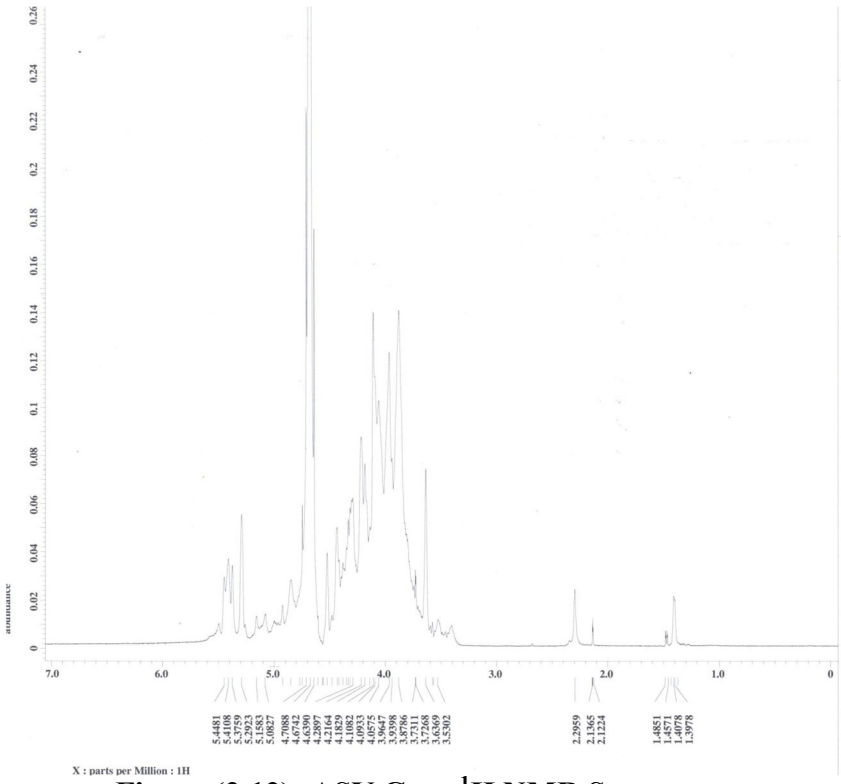

Figure (2.12): ASY Gum ^{1}H NMR Spectrum.

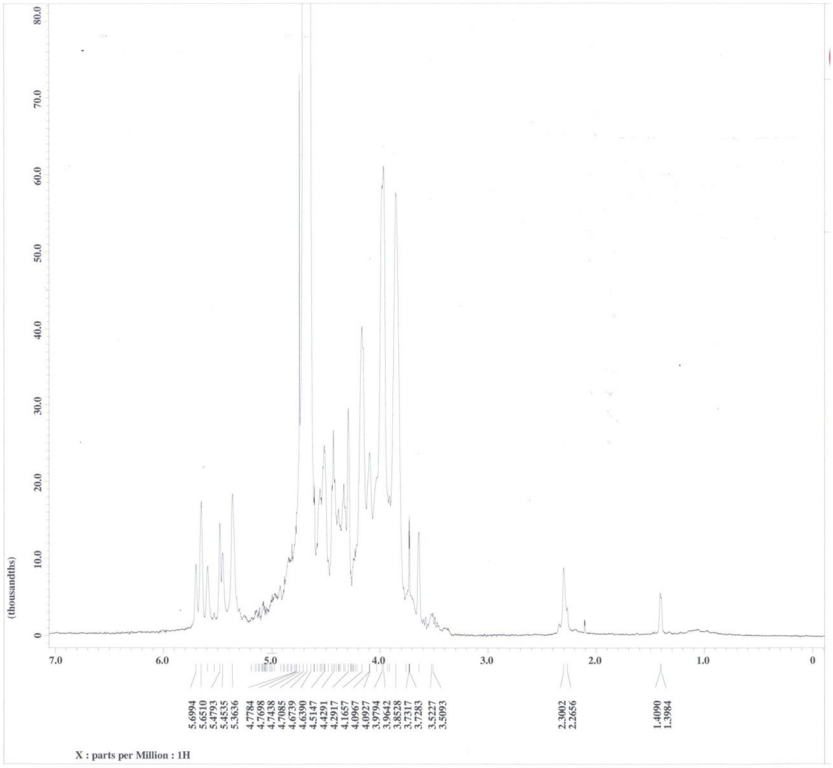

Figure (2.13): ATR Gum ^{1}H NMR Spectrum.

2.3.3. ATR-FTIR Spectroscopy

The FTIR spectra of ASG, AMF, ASY, and ATR gums (Fig. 2.14-2.17) depict a characteristic absorption band at 3290-3305 cm^{-1} representing the presence of hydrogen bonded OH group. The amino group which shows a characteristic absorption band in the region of 3400 - 3500 cm^{-1} must have been masked by an O-H group absorption band. The bands at 2926 cm^{-1} represent the presence of sugars, galactose, arabinose, and rhamnose, also the presence of alkane C-H stretch and aldehyde C-H stretch. The polymers also showed the characteristic band of C=C stretch, amide NH bend, NO_2 both from aliphatic and aromatic galactoproteins, and amino acids around 1602 cm^{-1}. The glucuronic acids have specific vibrations such as the band at 1411 and 1363 cm^{-1} due to C=O symmetric stretching and -OH bending, respectively. Alkane CH_3 bend, Aromatic C=C stretch, ketone C-C stretch, carboxylic acid C-O stretch, Anhydrides C-O stretch, Amine C-N stretch from Polysaccharides, Galactoproteins was observed at 1377 cm^{-1} band.1264cm^{-1} band represents alkane CH_3 bend, alcohol C-O stretch, ether C-O-C stretch, carboxylic acid CO stretch, amines C-N stretch alkyl due to sugar backbone showing alkane bend, alcohol stretch. Ether stretch is due to attachment of two galactose sugars. CO and CN stretches from galactoproteins. A distinct band at around 1029cm^{-1} represents alkene C-H bend from polysaccharides for all gum samples.

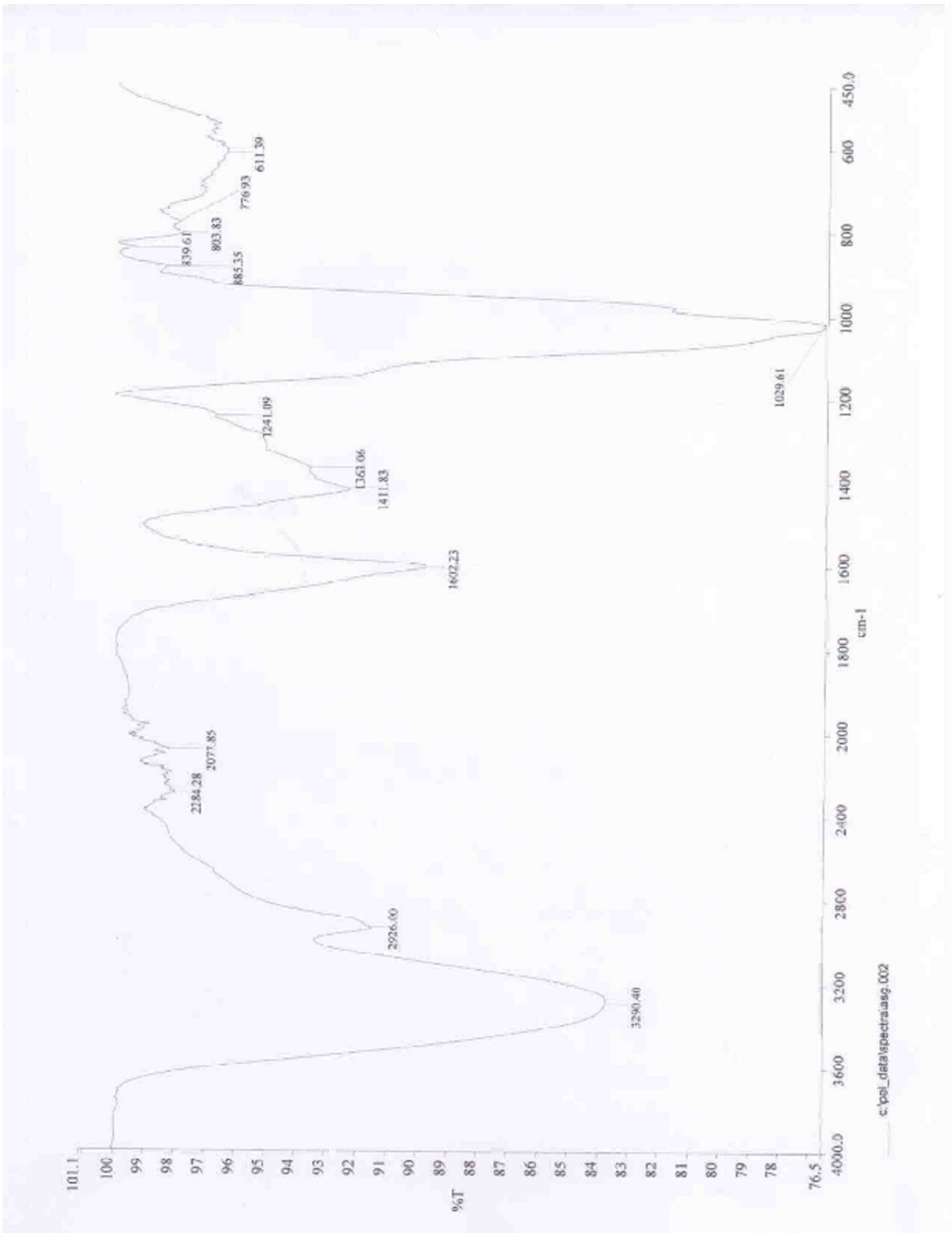

Figure (2.14): ASG Gum ATR-FTIR Spectrum.

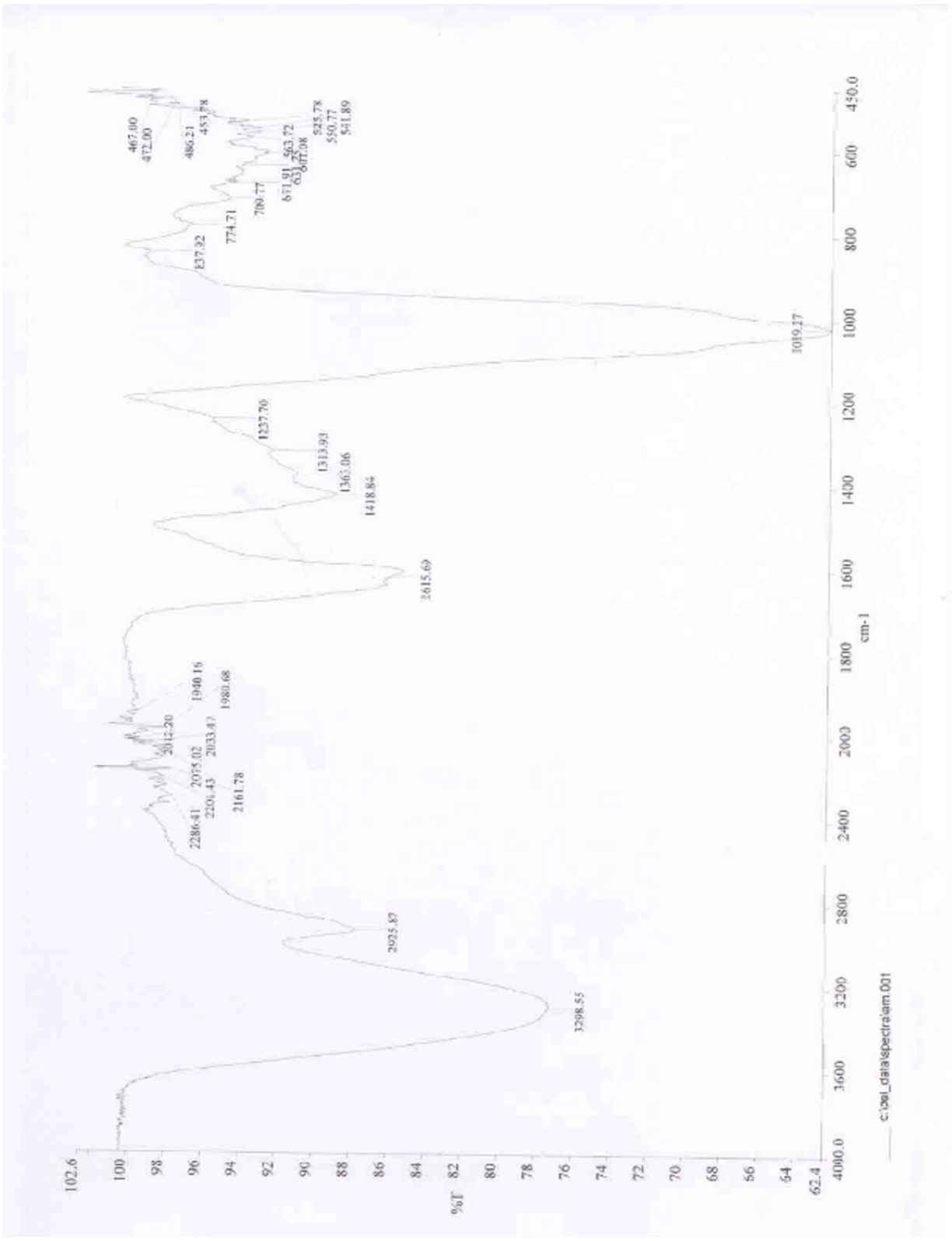

Figure (2.15): AMF Gum ATR-FTIR Spectrum.

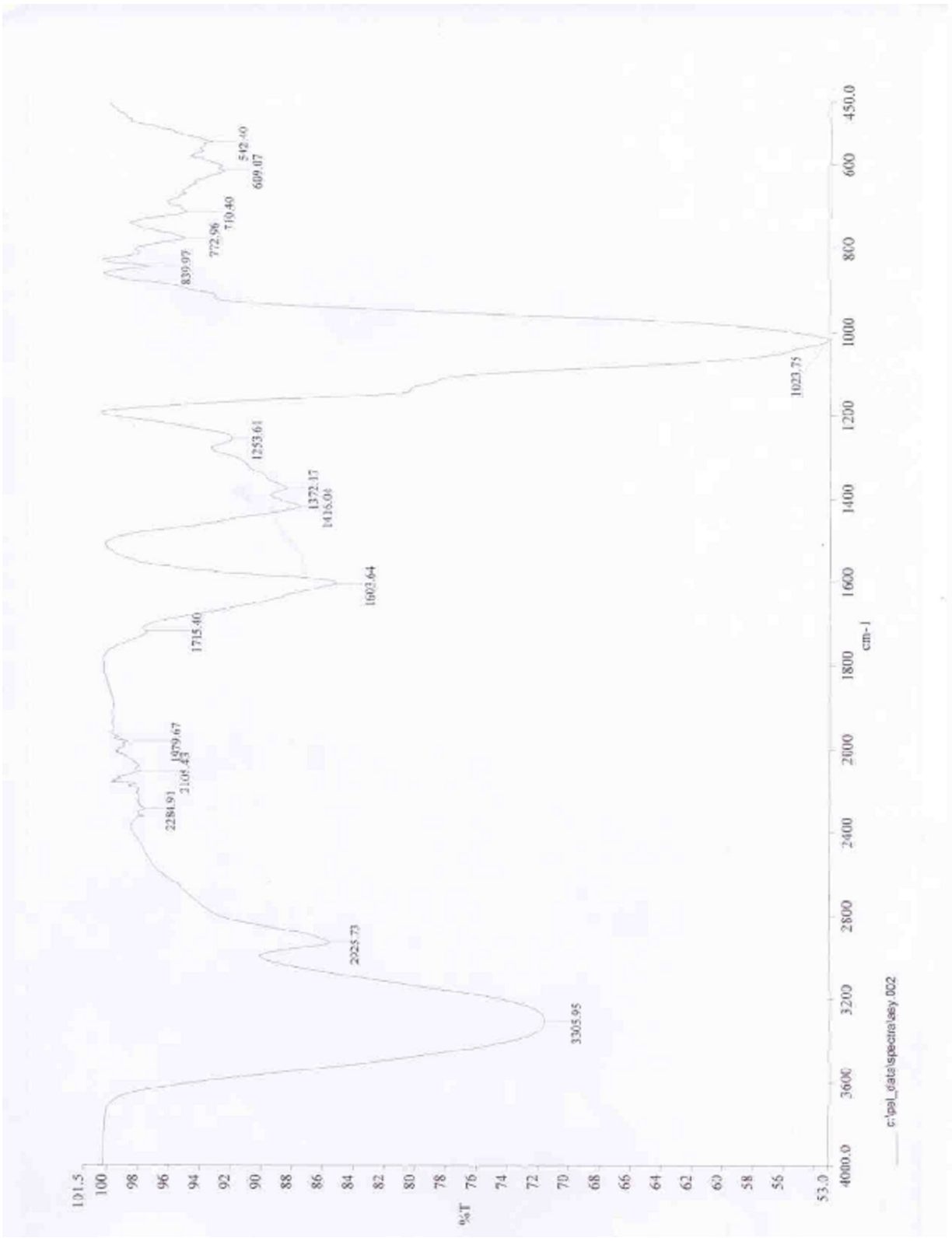

Figure (2.16): ASY Gum ATR-FTIR Spectrum.

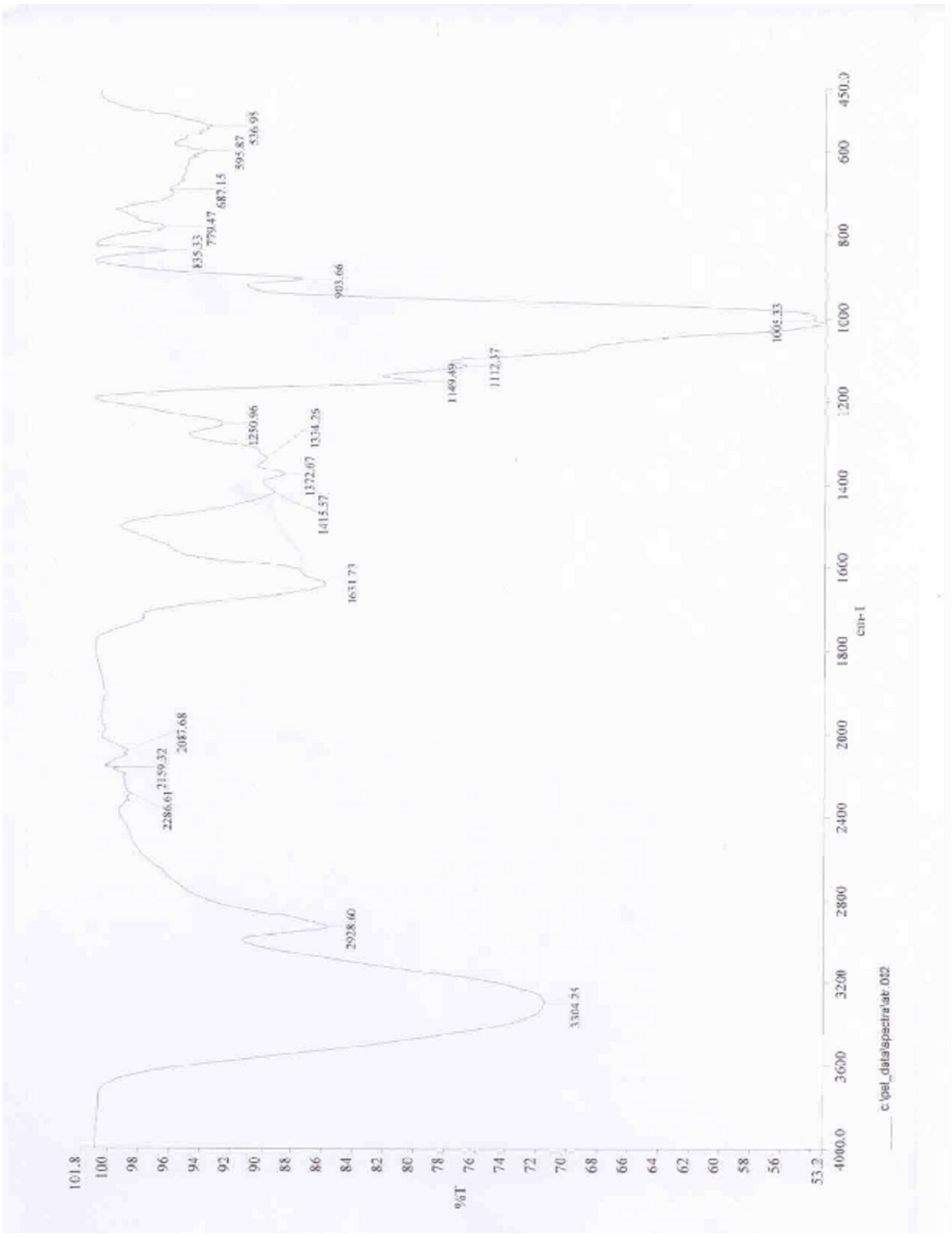

Figure (2.17): ATR Gum ATR-FTIR Spectrum.

The spectra of the studied gum samples were comparable and do not show noticeable differences from each other.

2.3.4. Thermal analysis

2.3.4.1. Differential Scanning Calorimetry (DSC)

Figures (2.18-2.21) show the DSC thermograms of ASG, AMF, ASY, and ATR gums. The thermogram of ASG gum (Figure 2.18) showed abroad endothermic beak and a beak temperature of 100 **C** which might be associated with a crystallization process followed by an exothermic beak associated to second favorable crystallization process with beak temperature of about 300 **C.** For AMF gum thermogram (Figure 2.19) the endothermic beak was sharp at around 150 **C** indicating a more crystal uniformity than ASG gum which exhibited broad endothermic beak which might be attributed to a less regular packing, and the exothermic beak at about 315 C. The ASY gum thermogram (Figure 2.20) showed endothermic beak at 150 **C** and exothermic beak at 300 **C.** The ATR gum thermogram (Figure 2.21) showed endothermic beak at 125 **C** and exothermic beak at 300 **C.**

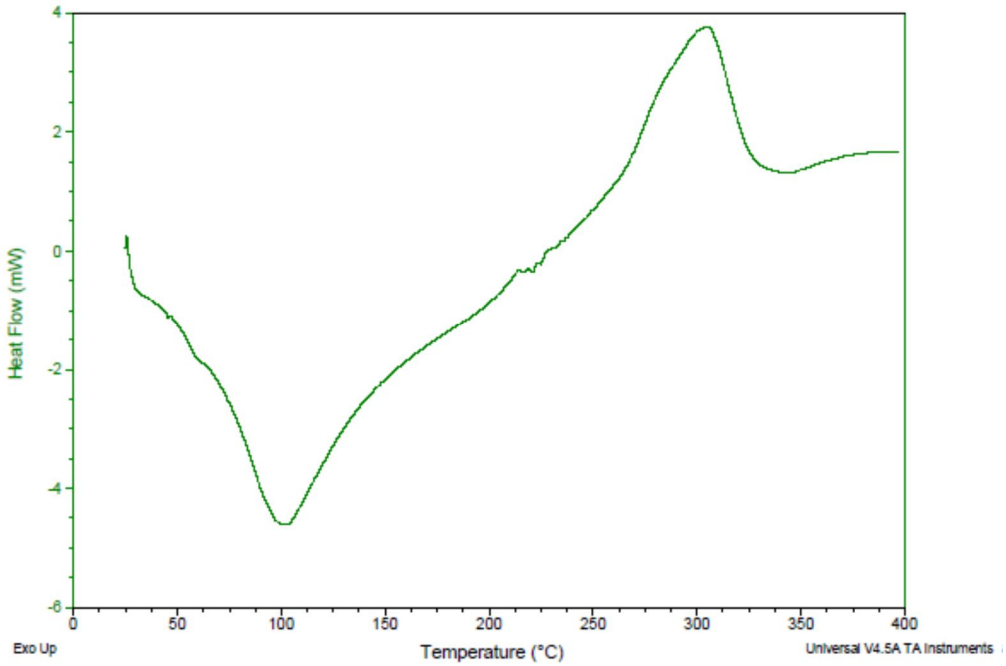

Figure (2.18): ASG Gum DSC Thermogram.

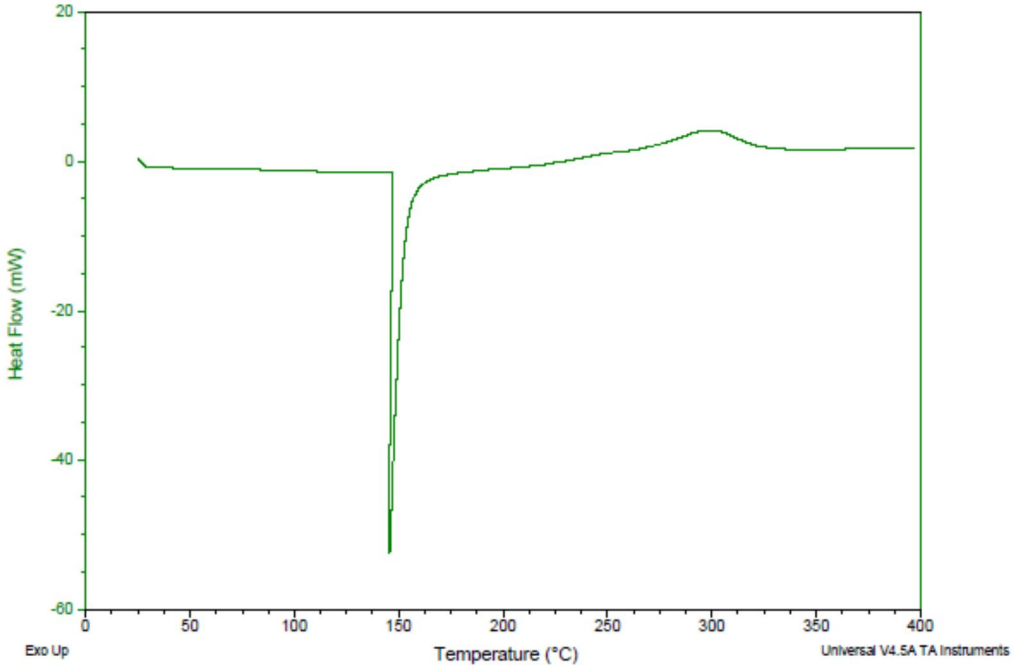

Figure (2.19): AMF Gum DSC Thermogram.

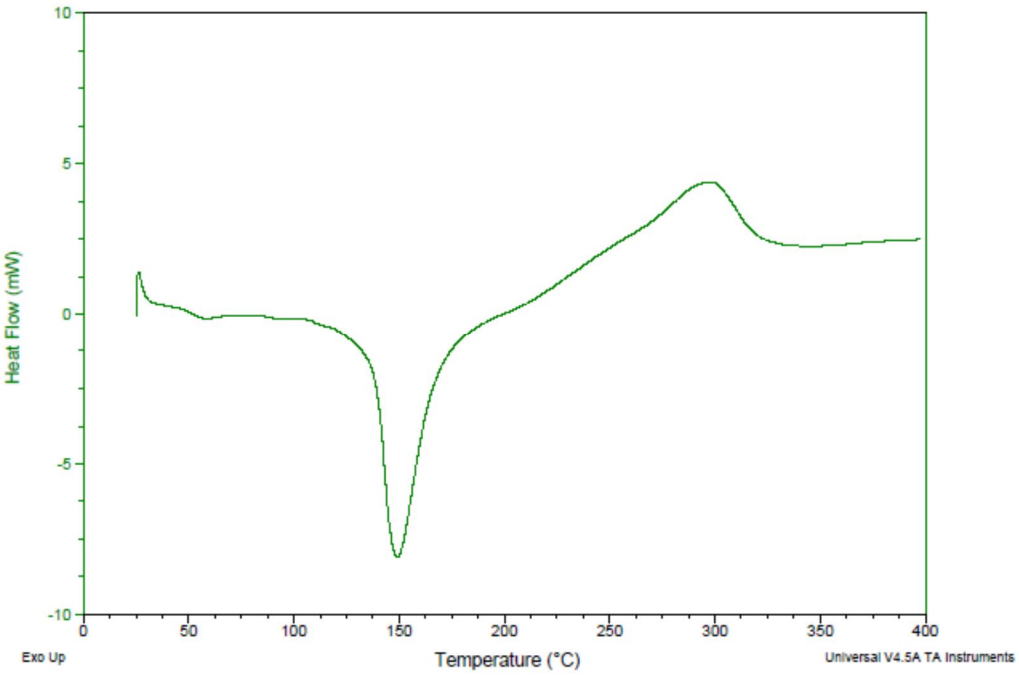

Figure (2.20): ASY Gum DSC Thermogram.

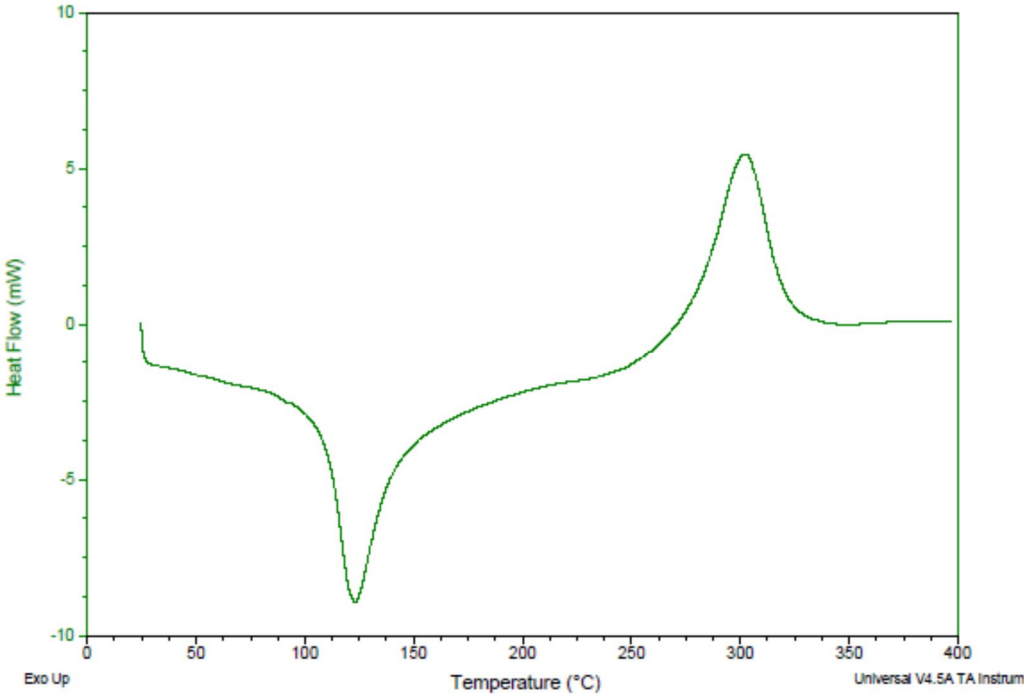

Figure (2.21): ATR Gum DSC Thermogram.

2.3.4.2. Thermogravimetric Analysis (TGA)

The representative plot results of thermogravimetric analysis carried out on the ASG, AMF, ASY, and ATR gum samples under nitrogen atmosphere are shown in Figures (2.22-2.25). The thermal analysis results are summarized in Table (2.3).

The details of thermal behavior and thermal stability data according to the primary thermograms and derivative thermograms for the gum samples show that heating at a rate of 10 **C** per minute from 30 **C** to a maximum of 400 **C** results in two mass loss events. The first mass loss, taking place between 30 -150 **C** is attributed to the loss of adsorbed and structural water of gums as related by other authors (Nep and Conway, 2010), or due to desorption of moisture as hydrogen-bound water to the polysaccharide structure. The second weight loss event with an onset of about 260 **C** resulted in a weight loss of about 60%, may be attributed to the polysaccharide decomposition (Zohuriaan and Shokrolahi, 2004) and is described by a weight loss onset of 260.8 **C** and a maximum oxidation temperature of 318.2 **C** for ASG gum. The mass residue of the gums was about 30-35%. The weight loss onset (representing the onset of oxidation or decomposition) of 260.8 **C** suggests that polysaccharide gums has good thermal stability.

The onset temperatures associated with the second mass loss were characteristic for the different gum samples imply different gum origin.

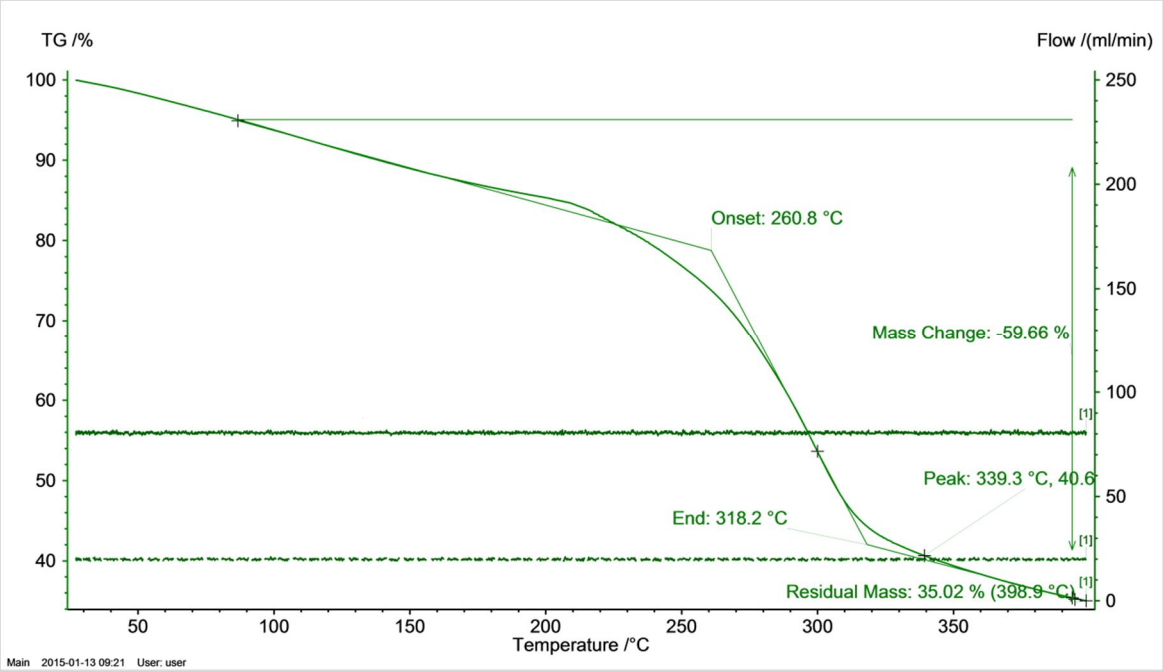

Figure (2.22): ASG Gum TGA Thermogram.

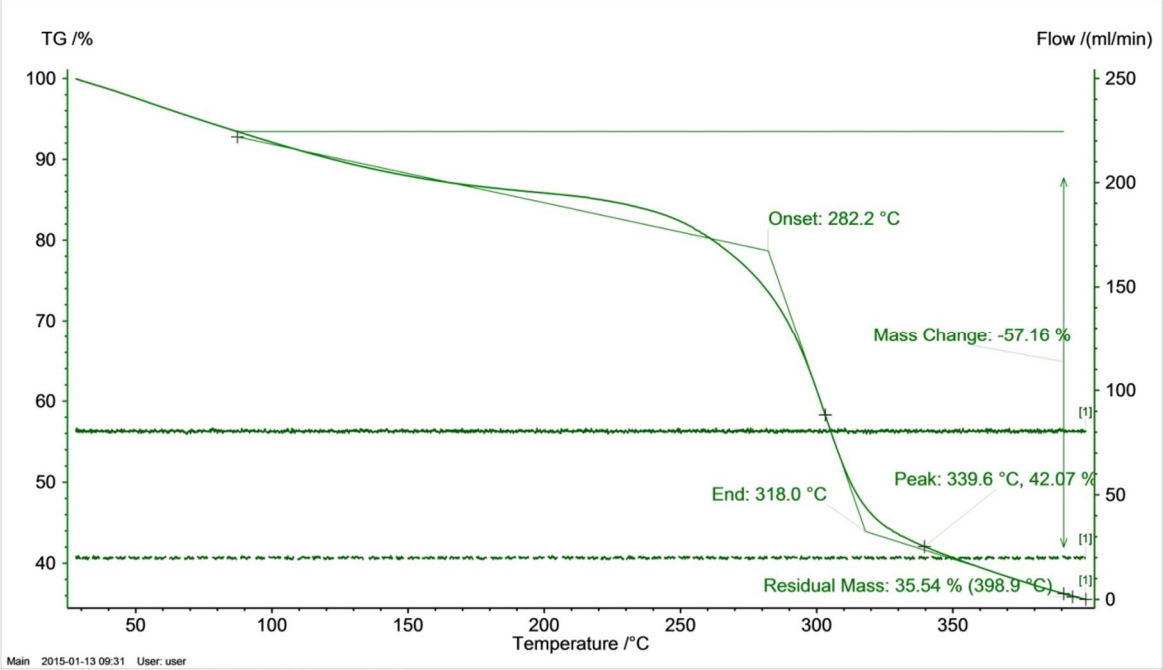

Figure (2.23): AMF Gum TGA Thermogram.

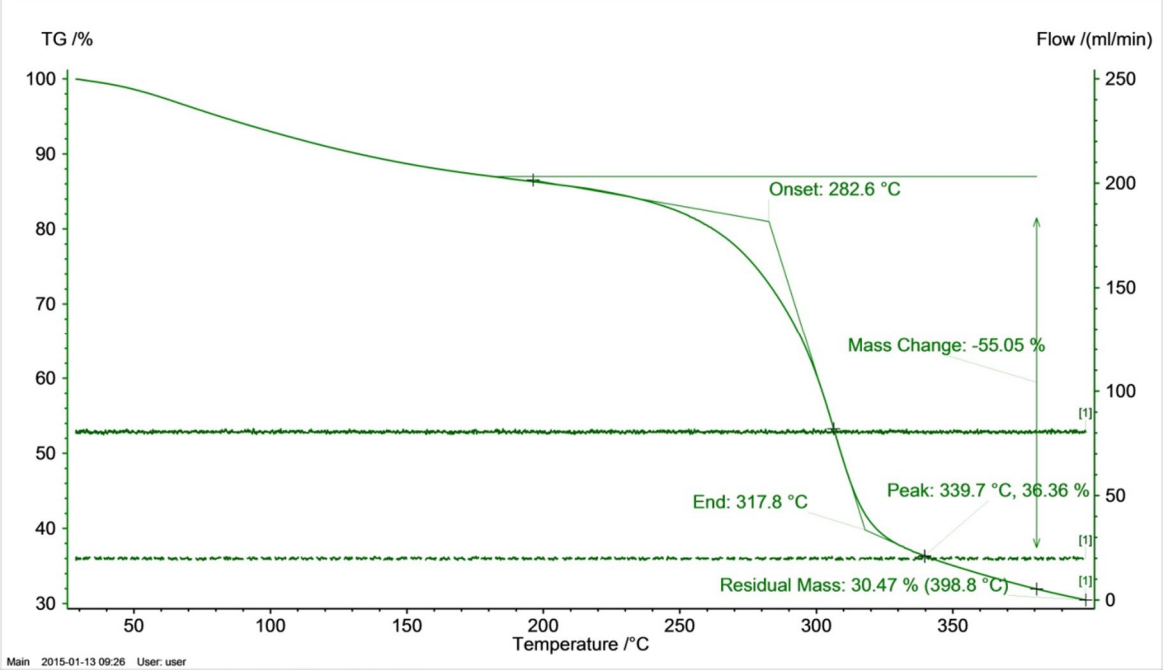

Figure (2.24): ASY Gum TGA Thermogram.

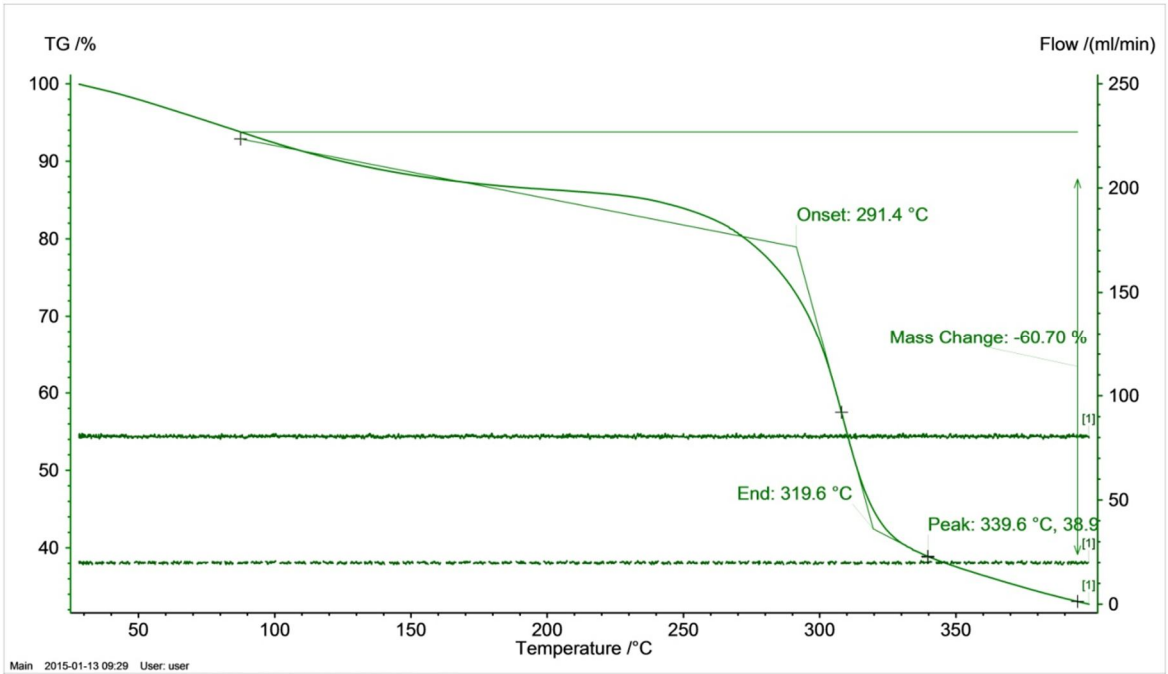

Figure (2.25): ATR Gum TGA Thermogram.

Table 2.3. Thermal decomposition data for the different gum samples.

Gum Sample	T_0 (C)[a]	$T_{max.}$ (C)	% Mass loss
ASG	260.8	339.2	59.66
AMF	282.2	339.6	57.16
ASY	282.6	339.7	55.05
ATR	291.4	339.6	60.70

[a]T_0: onset temperature.

2.4. Conclusions

- Although gum samples showed similarities in functional groups; which were clear from the NMR and ATR-FTIR results, the DSC and TGA thermograms were characteristic for each gum and the NMR results reflected different gums structures noticed from the characteristic spectrum for each gum.
- Also the gums showed different physicochemical properties reflecting the variations between the *Vulgares* and *Gummiferae* series, and further the variations between the species. These differences could be summarized as follows;

- While gums from *Vulgares* series (ASG and AMF) showed negative optical rotation, *Gummiferae* series gums (ASY and ATR) were positively rotating the polarized light.
- The nitrogen and consequently the protein contents were different even within the same series; this was seen from the high protein content of the ATR gum from the Gummiferae series and the very low protein content of ASY gum from the same series.
- The number average molecular weight was higher for the *Gummiferae* gums than for *Vulgares* gums.